C. R. Physique 19 (2018) 710–720

Contents lists available at ScienceDirect

Comptes Rendus Physique

www.sciencedirect.com

New trends in metallic alloys / Alliages métalliques : nouvelles tendances

Design of strain-transformable titanium alloys

Conception d'alliages de titane transformables par déformation

Philippe Castany [a,*], Thierry Gloriant [a], Fan Sun [b,*], Frédéric Prima [b]

[a] *Univ Rennes, INSA de Rennes, CNRS, ISCR, UMR 6226, 35000 Rennes, France*
[b] *PSL Research University, Chimie ParisTech–CNRS, Institut de recherche de Chimie Paris, 75005 Paris, France*

ARTICLE INFO

Article history:
Available online 15 October 2018

Keywords:
Titanium alloys
Metastable β phase
Superelasticity
TRIP
TWIP

Mots-clés :
Alliages de titane
Phase β métastable
Superélasticité
TRIP
TWIP

ABSTRACT

Amongst titanium alloys, metastable β types are the most promising to improve performances of materials currently used in several sectors such as aeronautics or biomedical applications. Particularly, some metastable β titanium alloys exhibit a stress-induced martensitic transformation (into the orthorhombic α″ phase) that can be tuned to obtain superelasticity or the TRansformation Induced Plasticity (TRIP) effect. The design strategy of such strain-transformable alloys is presented here, and some recent key findings are highlighted and discussed.
© 2018 Académie des sciences. Published by Elsevier Masson SAS. This is an open access article under the CC BY-NC-ND license (http://creativecommons.org/licenses/by-nc-nd/4.0/).

RÉSUMÉ

Parmi les alliages de titane, ceux de type β métastable sont les plus prometteurs pour améliorer les performances des matériaux utilisés actuellement dans de nombreux secteurs tels que l'aéronautique ou le biomédical. En particulier, certains alliages de titane β métastable sont sujet à une transformation martensitique induite sous contrainte (vers la phase α″ orthorhombique), qui peut être ajustée afin d'obtenir de la superélasticité ou un effet TRIP (*TRansformation-Induced Plasticity*). La stratégie de conception de ces alliages transformables par déformation est présentée ici et quelques découvertes majeures récentes sont mises en lumière et discutées.
© 2018 Académie des sciences. Published by Elsevier Masson SAS. This is an open access article under the CC BY-NC-ND license (http://creativecommons.org/licenses/by-nc-nd/4.0/).

1. Introduction

Titanium alloys are widely used in aeronautics due to their high strength/density ratio and for biomedical applications due to their good biocompatibility. Amongst titanium alloys, metastable β titanium alloys are more and more considered because of the wide panel of mechanical properties that can be obtained. In such alloys, the β phase (bcc structure), which is the stable phase of pure titanium at high temperature, is the main or the sole constituent phase of the microstructure. This

* Corresponding authors.
E-mail addresses: philippe.castany@insa-rennes.fr (P. Castany), fan.sun@chimieparistech.psl.eu (F. Sun).

https://doi.org/10.1016/j.crhy.2018.10.004
1631-0705/© 2018 Académie des sciences. Published by Elsevier Masson SAS. This is an open access article under the CC BY-NC-ND license (http://creativecommons.org/licenses/by-nc-nd/4.0/).

phase is retained at room temperature by addition of β-stabilizer elements (V, Cr, Nb, Mo...) and quench from the high-temperature β domain in order to keep a metastable state. Due to its metastable nature, the β phase can be subject to phase transformations allowing a fine design of the microstructure and of the subsequent mechanical properties. As an example, fine precipitation of the stable α phase (hcp) can be obtained after heating in the α + β domain to reach high strength in the Ti5553 alloy, currently used for landing gear structures of modern airplanes [1]. Another way to promote high strength is to precipitate the ω phase after aging at moderate temperature: this metastable phase precipitates as nanometer-sized particles homogeneously distributed in β-phase grains [2–7]. Finally, the metastable β phase can also transform into an orthorhombic phase, namely α″, when a stress is applied. This stress-induced martensitic (SIM) transformation is of special interest because it can lead to the TRansformation-Induced Plasticity (TRIP) effect, promoting high ductility and strain hardening [8–12], or superelasticity when this SIM transformation is reversible promoting thus high recoverable strain [13–18]. These two properties will be more precisely developed in the present paper.

2. Superelastic titanium alloys

2.1. Motivation towards the development of new superelastic Ti alloys

During the last decade, the increase of superelasticity, i.e. the recoverable strain after deformation, was one of the main goals of the design of new superelastic metastable β titanium alloys. Indeed, superelasticity is a property requested for some biomedical devices such as stents, orthodontic arch wires, or catheter guides. However, such superelastic biomedical devices are actually made from near-equimolar NiTi alloys (Nitinol), which cause problems due to the presence of nickel because of its allergenic effect for an increasing part of the population [19–21]. As metastable β titanium alloys can be made only from highly biocompatible elements (such as Nb, Mo, Ta, Zr, Sn...), these alloys are thus promising candidates to replace NiTi alloys as Ni-free superelastic alloys. Since recently, niobium was used as the main alloying element, but binary Ti–Nb alloys exhibit quite poor properties with low recoverable strain and low strength [13]. Several ways can thus be used to increase the superelasticity of binary Ti–Nb alloys, and the simplest one is to change alloy composition by adding other alloying elements with the aim of a twofold effect. The first one is to decrease the value of the martensite start temperature below the room temperature in order to have a superelastic effect. The second one is to increase, by a solute hardening effect, the critical stress of mechanisms of plasticity, namely dislocation slip and also twinning, which often occurs in this type of alloys. Indeed, the recoverable strain is limited if plasticity occurs due to the trapping of stress-induced martensite (SIM) by dislocations and/or twins. SIM can thus not totally transform back into the β phase when the stress is released, leading to a decrease in recoverable strain. For example, an increase in Ta [22] or Zr [23] content in Ti–Nb–based alloys allows a superelasticity increase related to an increase in the critical stress of the mechanisms of plastic deformation. Another way to increase the critical stress for plasticity is to reduce the grain size by performing a short heat treatment after cold working in order to limit grain growth during the recrystallization process [24–26]. Precipitation of a nano-sized ω phase during a low-temperature aging can also be performed to reach the same result [13,16]. Finally, the control of the crystallographic texture is maybe the most important parameter. Indeed, the transformation strain is very dependent on the direction of the tensile stress regarding the β phase structure [13,27]. The ideal transformation strain can be calculated for each crystallographic direction of the applied strain when a β-phase single crystal is totally transformed into the single variant of α″ martensite that accommodates the maximum of strain. The results of this calculation can be plotted in an inverse pole figure highlighting the maximum transformation strain as a function of the tensile direction in a β-phase single crystal. An example is shown in Fig. 1 for the Ti–24Nb–4Zr–8Sn (wt.%) alloy [27]. The general trend is common for all metastable β titanium alloys, as it only depends on the crystallography of both β and α″ phases: the maximum value of the recoverable strain is obtained for tensile directions along ⟨110⟩ directions, while the lowest value is achieved for ⟨111⟩ directions. Conversely, the values of transformation strains depend on the lattice parameters of both phases and, in turn, on alloy composition. These values for the tensile direction along the three main crystallographic directions are then expressed as:

$$\frac{b_{\alpha''} - \sqrt{2}a_\beta}{\sqrt{2}a_\beta} \quad \text{for } \langle 110\rangle_\beta \qquad \frac{\frac{\sqrt{b_{\alpha''}^2 + c_{\alpha''}^2}}{2} - a_\beta}{a_\beta} \quad \text{for } \langle 100\rangle_\beta \qquad \frac{\sqrt{a_{\alpha''}^2 + b_{\alpha''}^2} - \sqrt{3}a_\beta}{\sqrt{3}a_\beta} \quad \text{for } \langle 111\rangle_\beta$$

where a_β is the lattice parameter of the bcc β phase and $a_{\alpha''}$, $b_{\alpha''}$, $c_{\alpha''}$ are the ones of the α″ orthorhombic martensite.

For polycrystalline materials, the best superelastic properties are thus obtained from strongly textured materials with ⟨110⟩ directions along the tensile direction. This type of texture is obtained after recrystallization of cold-worked materials with a precise adjustment of both cold-working rate and temperature/time of the following heat treatment [15,26,28,29]. Therefore, getting the optimal texture is the first step to achieve the best superelasticity of a given alloy composition. Next, other parameters can be optimized to improve again the recoverable strain, such as increasing the critical stress for plastic deformation mechanisms.

Understanding the deformation mechanisms occurring in superelastic β metastable titanium alloys is also of key interest to improve their properties. SIM transformation is the most important mechanism responsible for superelasticity but, due

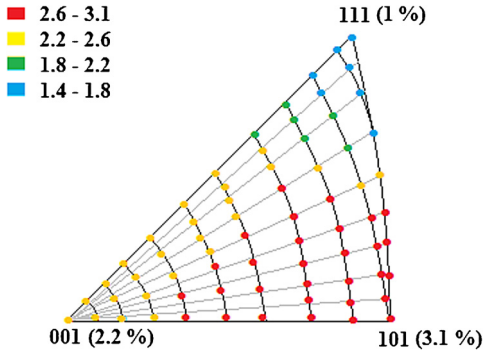

Fig. 1. Orientation dependence of the maximum transformation strain associated with the β-to-α″ martensitic phase transformation in the Ti–24Nb–4Zr–8Sn alloy [27].

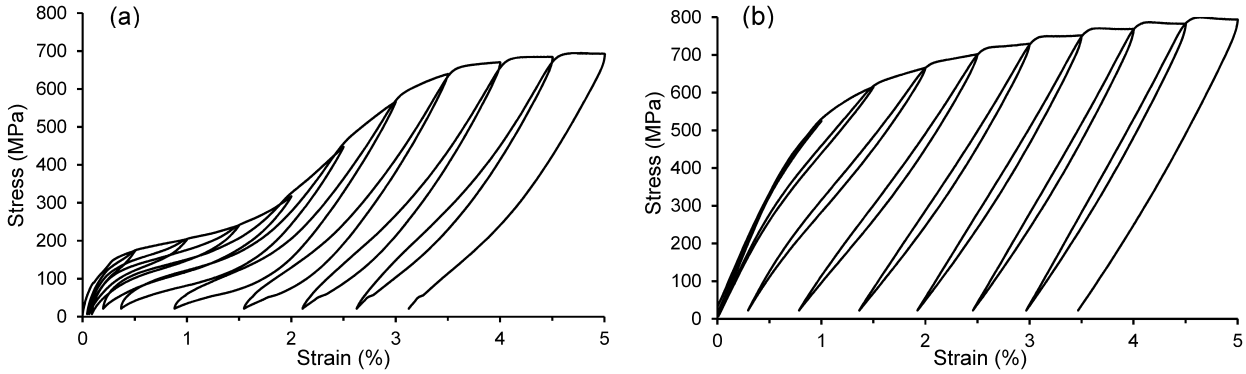

Fig. 2. Cyclic stress–strain curves of Ti–24Nb–0.5N (a) and Ti–24Nb–0.5O (b) alloys.

to its reversible nature, only *in situ* experiments under stress can be used to characterize this mechanism. *In situ* X-ray diffraction is thus mainly used, with a special interest in synchrotron radiation [17,18,30,31]. However, the study of plastic deformation mechanisms is also of great interest, because the increase of their critical stress is a way to improve the recoverable strain. Indeed, limiting dislocations or twin activities avoids trapping of SIM and thus improves the recoverable strain. Some recent findings about the three mechanisms of deformation occurring in these alloys, i.e. SIM transformation, dislocation slip, and twinning, will thus be highlighted in the following section.

2.2. Some highlights on superelastic alloys

2.2.1. Reversible SIM transformation

Superelastic metastable β titanium alloys can exhibit two types of tensile stress–strain curves: the most classical one shows an obvious stress plateau related to the SIM transformation, while tensile curves of some alloys do not exhibit such a stress plateau. These two behaviors are illustrated in Fig. 2 for two alloys with very close compositions [17]. Superelasticity is then evaluated from the recoverable strain, which is measured from cyclic tensile tests. These tests consist of strain increments followed by a total release of the stress after each step. The cyclic tensile curve of the Ti–24Nb–0.5N (at.%) alloy evidences thus a classical behavior with a stress plateau and occurrence of hysteresis between loading and unloading curves (Fig. 2a). Conversely, the cyclic tensile curve of the Ti–24Nb–0.5O (at.%) alloy does not exhibit a stress plateau, but hysteresis appears for strains higher than the yield point (Fig. 2b). Despite these differences, the superelasticity of both alloys is similar: 2% for the Ti–24Nb–0.5N alloy and 2.2% for the Ti–24Nb–0.5O alloy [32]. It can also be noticed that both alloys have the same crystallographic texture with the optimal ⟨110⟩ direction along the tensile direction [17]. Therefore, their different behaviors cannot be explained by texture variations. If the SIM transformation seems obviously to happen in the Ti–24Nb–0.5N alloy, its occurrence is debatable in the Ti–24Nb–0.5O alloy. That is why the same cyclic tensile tests are conducted *in situ* under synchrotron radiation in order to elucidate the reversible mechanisms responsible for the superelasticity of these alloys.

Synchrotron X-ray diffractograms (SXRD) obtained during cyclic tensile tests of Ti–24Nb–0.5N and Ti–24Nb–0.5O alloy are presented in Fig. 3 for each cycle, under load and after removing the stress. Due to the strong ⟨110⟩ texture of both alloys and the geometry of the setup, only the $\{110\}_\beta$ peak is initially detected (as well as the second order $\{220\}_\beta$) [17]: the diffractograms are thus focused around this peak for a better readability. As assumed from the cyclic tensile curve, the SXRD of the Ti–24Nb–0.5N alloy reveals classical superelastic behavior (Fig. 3a). First, the elastic deformation of the β

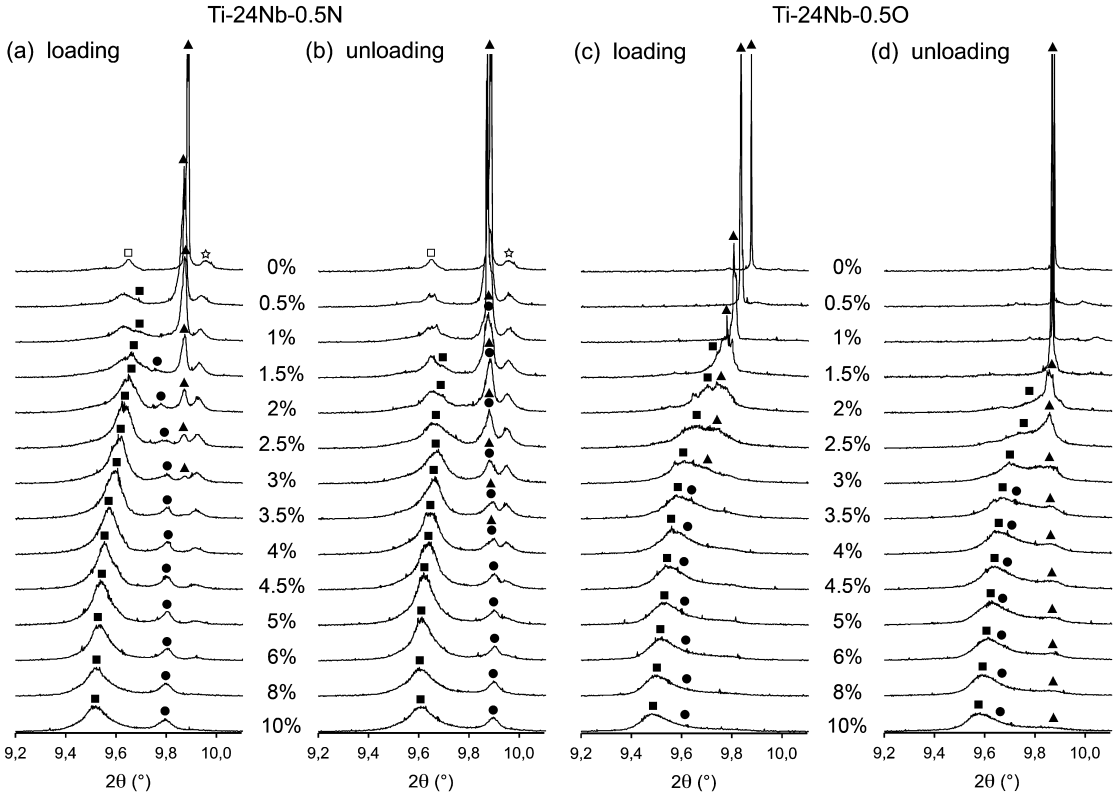

Fig. 3. SXRD profiles around the $\{110\}_\beta$ peak (black triangles) acquired during *in situ* cyclic tensile tests under loading (a, c) and after unloading (b, d) for both Ti–24Nb–0.5N and Ti–24Nb–0.5O alloys; the corresponding strain of each cycle is indicated beside each pattern. Squared symbols label $(020)_{\alpha''}$ peaks, circles label $(002)_{\alpha''}$ peaks and stars label $(111)_{\alpha''}$ peaks; open symbols correspond to a small amount of α'' phase formed during quenching.

phase occurs, which is highlighted by the shift of the $\{110\}_\beta$ peak (black triangle) for 0.5% of strain under load. Then, this peak remains at the same position, and its intensity continuously decreases until its complete vanishing for 3% of strain. At the same time, the $(020)_{\alpha''}$ and $(002)_{\alpha''}$ peaks of martensite (black squares and black circles, respectively) appear with progressively increasing intensities, showing the occurrence of SIM transformation. After unloading (Fig. 3b), the intensities of the α'' peaks are lower than under load, while the intensity of the β peak is higher, revealing the reversible nature of the SIM transformation. These results show thus that the superelasticity of the Ti–24Nb–0.5N alloy is due to the occurrence of the reversible β to α'' SIM transformation.

The SXRD results of the Ti–24Nb–0.5O alloy show some different features: the $\{110\}_\beta$ peak continuously shifts until its complete vanishing for 3% of strain (Fig. 3c), whereas the peaks of α'' martensite appear from 1% of applied strain. After unloading, as for the Ti–24Nb–0.5N alloy, the shift of the β peak is reversible, and the intensities of the α'' peaks decrease (Fig. 3d). These results highlight an unusual behavior, with an important elastic deformation of the β phase and its concomitance with a reversible SIM transformation. The recoverable strain of this alloy is then due to the combination of a huge elasticity of the β phase and of the reversible β-to-α'' SIM transformation, which leads to the absence of stress plateau on tensile curves. This unusual behavior can also be observed in some other alloys, and is attributed to a relatively high oxygen content [18,31,33].

2.2.2. Plastic deformation mechanisms

The plasticity of metastable β titanium alloys is generally accommodated by both dislocation slip and twinning. Twinning was more deeply investigated as discussed hereafter, while specific studies of dislocations are fewer. Dislocation slip and features of dislocations' mobility were recently studied from *in situ* tensile tests performed in Transmission Electron Microscopy (TEM) [34–37] or other experimental techniques [38,39] and atomistic simulations [40,41]. All these studies show that dislocations have the usual behavior of dislocations in bcc metals and alloys with dislocations with $a/2\langle 111\rangle$ Burgers vector gliding mainly in {110} and {112} planes [34–38] and sometimes in {123} planes [35,36]. The deformation rate is then controlled by the low mobility of screw dislocations due to a strong Peierls stress related to the core structure of these screw dislocations [34–38,40,41].

Twinning was more investigated in metastable β titanium alloys, mainly due to the occurrence of a peculiar twinning system of bcc alloys. Indeed, the $\{332\}\langle 113\rangle$ twinning system is mainly activated instead of the classical $\{112\}\langle 111\rangle$ twinning system that is observed in all other bcc metals and alloys. Occurrence of one or both twinning systems is very dependent on

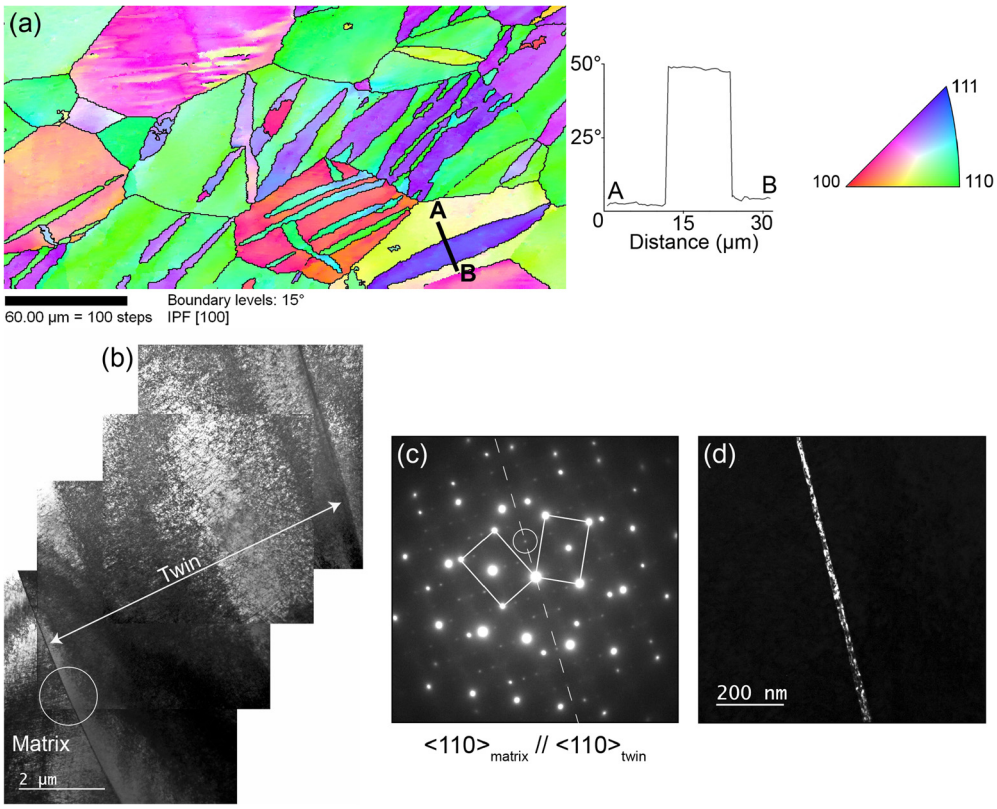

Fig. 4. (a) EBSD–SEM inverse pole figure map showing {332}⟨113⟩ twins after deformation in a Ti–27Nb alloy and (b) TEM bright field image of the same type of twin; (c) SAED pattern showing the twinning relationship and (d) a dark field image of the region circled in (a) with the spot circled in (c).

the alloy composition and the unusual {332}⟨113⟩ twinning system is observed in the most unstable alloys [42–44], including superelastic ones [32,35,37,45]. Since the first identification of this unique twinning system in 1971 [46], its occurrence was related to the β-to-α″ SIM transformation, but the formation mechanisms were still unknown. Its origin was elucidated recently by combining several techniques in a Ti–27Nb (at.%) superelastic alloy [47]. As shown in the previous section for the two Ti–24Nb–0.5N and Ti–24Nb–0.5O alloys from *in situ* SXRD experiments, the present Ti–27Nb alloy is also totally transformed into α″ martensite from about 3% of applied strain [47], which is similarly visible from the total vanishing of β peaks in the SXRD profiles of the Ti–24Nb–0.5N and Ti–24Nb–0.5O alloys (Figs. 3a and 3c). However, twinning is an irreversible mechanism of deformation that appears at higher strain, therefore when no more β phase is present in the material. But, as the SIM transformation is reversible in superelastic alloys, {332}⟨113⟩ twins can be evidenced in the β phase after deformation by EBSD or TEM (Figs. 4a and 4b), even if these twins are in fact formed into α″ martensite under stress. These results prove unambiguously that {332}⟨113⟩ twins are not formed in the β phase, but are the resultant of the reversion of twins formed into the SIM α″ phase [47]. From TEM analysis (Fig. 4c) and crystallographic reconstruction, the real twinning system activated in the α″ phase is found to be the new $\{130\}\langle 310\rangle_{\alpha''}$ one [47]. The occurrence of this new twinning system was further confirmed from direct observations [48,49]. Finally, due to this reversion process, the {332}⟨113⟩ twin boundary often exhibits features related to stress relaxation occurring during the α″-to-β reverse phase transformation such as a thin layer of ω phase as shown in Fig. 4d, where a thin layer of ω phase along the twin boundary is visible on the dark-field image taken from the additional spot of the ω phase circled in the selected area electron diffraction (SAED) pattern of the Fig. 3c. It can also be noticed that a similar process can lead to the formation of the classical {112}⟨111⟩ twinning system, as recently shown in a superelastic Ti–24Nb–4Zr–8Sn single crystal, which also totally transforms into α″ martensite during deformation [50]. In such a case, the twinning system in α″ martensite is $\{110\}\langle 110\rangle_{\alpha''}$, and the reversion is also accompanied with the formation of a thin layer of ω phase along the twin boundary during the reverse phase transformation. If the origin of {332}⟨113⟩ twins (and {112}⟨111⟩ twins to lesser extent) in superelastic alloys is now unambiguously demonstrated, the situation is still too complex to be understood in non-superelastic alloys. Indeed, as the β phase is not totally transformed into α″ martensite during deformation and as the SIM α″ can be partially reversible, it is not obvious to conclude if the {332}⟨113⟩ twins are only due to the reversion of $\{130\}\langle 310\rangle_{\alpha''}$ twins occurring in α″ or if they are directly formed into the β phase or more probably start to form into α″ plates and propagate in the surrounding β phase. Further investigations are needed to totally explain the origin of this peculiar {332}⟨113⟩ twinning system in such alloys.

2.3. Perspectives to improve superelasticity

New findings on mechanisms of deformation occurring in superelastic metastable β titanium alloys were reported during these last years. The development of *in situ* tensile tests under synchrotron X-ray radiation allowed a better understanding of the SIM transformation and of the sequence of deformation. However, most of the alloys investigated contain niobium as the main alloying element, and these alloys exhibit a recoverable strain limited to around 3%. In order to obtain titanium alloys with recoverable strains higher than 3%, a new strategy is to replace niobium as the main alloying element by zirconium [29,51] or hafnium [52]. Relatively high contents of Zr or Hf lead to increase the lattice parameters of both β and α″ phases and, in turn, to increase the transformation strain (as discussed in section 2.1). Another strategy, few developed until now, is to start with a shape-memory alloy, i.e. fully composed of α″ martensite in the initial state, and perform a low-temperature aging treatment above the austenite finish temperature and within the temperature domain of ω phase formation. With an appropriate aging time, ω-phase precipitation can impede the formation of α″ martensite during further cooling and thus can allow one to obtain a full β phase material that exhibits higher recoverable strain due to its higher instability [53].

The mechanisms of plastic deformation occurring in α″ martensite have only been explored for a few years, while their precise knowledge is also essential to delay the activation process and thus to improve the recoverable strain. However, their characterization is quite challenging due to the reversibility of the SIM α″ transformation. In order to overcome this difficulty, the mechanisms of deformation are investigated from plastically deformed shape-memory alloys, which are only composed of α″ martensite and for which the α″ to β transformation does not occur when the stress is released. This approach was successfully applied to find new twinning systems of α″ martensite [48,49] and would allow a better understanding of the deformation of α″ phase.

3. TRIP/TWIP titanium alloys

3.1. Motivations towards development of new strain transformable titanium alloys

The use of β titanium alloys in advanced applications [54–56] is, however, still delayed by remaining drawbacks, such as limited ductility, strain hardening, or damage resistance. The development of this new family of titanium alloys referred to as TWIP/TRIP Ti alloys is initially motivated by the great need to fill new areas in the mechanical properties space, using a controlled combination of stress-induced transformations such as mechanical twinning and stress-induced phase transformation [8,57,58]. The main targeted property is currently the strain-hardening rate, which is known to be either low or non-existent in titanium alloys (Fig. 5). Besides, positive consequences from strain-hardening improvement are expected on ductility and damage tolerance, respectively.

Challenges are multiple, including: (i) the consistent choice of a design approach, (ii) the considerable lack of information regarding both martensitic transformation and mechanical twinning viewed as efficient plastic deformation mechanisms, in titanium alloys, (iii) the hidden complexity of new materials displaying both simple chemical composition and simple (single-phase) initial microstructures but incredibly complex deformed microstructures, even in the small deformation range [8,9,47].

3.2. Design approach of TWIP/TRIP titanium alloys

The first question asked regarding the development of TRIP/TWIP alloys is related to the design strategy. Being established that chemical and mechanical stabilities are closely related in titanium alloys, the question is then firstly reduced to the fine control of the chemical stability of the β phase. Historically, the molybdenum equivalent (Mo_{eq}) criterion has been used as the most common empiric rule to scale the relative stability of titanium alloys and to divide titanium alloys into three distinct families (α, α+β, β). However, despite its industrial usefulness, this parameter has been shown to be more indexed on the alloying influence with respect to the T_β temperature (transition temperature between the α and β phases) than properly on the stabilization level of the respective alloying elements with respect to the β phase itself.

In the early 1990s, Morinaga and colleagues [57,58] proposed a new method for theoretical alloy design, on the basis of molecular orbital calculations of the electronic structure (DV–Xα cluster method) [59,60]. This method was initially used as a guiding tool for Ti alloys design with superelastic properties, based on the phase stability prediction of β phase [60,61]. Based on electronic structures calculations on a 15-atom BCC Ti cluster, two theoretical parameters, signing respectively the cohesion force and the chemical stability of the cluster, are evaluated: The bonding order (B_o), the measure of the covalent bond strength between Ti and alloying elements; and the mean d-orbital energy level (M_d), which correlates with the electronegativity and the metallic radius of elements. In that way, starting from a pure Ti cluster, the electronic perturbation associated with most of the possible alloying elements can be quantitatively evaluated with respect to these two stability parameters. For multi-component alloys, the values of B_o and M_d are defined by taking the compositional averages of the parameters, denoted as $\overline{B_o}$ and $\overline{M_d}$. The electronic parameters $\overline{B_o}$ and $\overline{M_d}$ for each alloy were calculated from the following expressions:

$$\overline{M_d} = \sum X_i (M_d)_i \quad \text{and} \quad \overline{B_o} = \sum X_i (B_o)_i$$

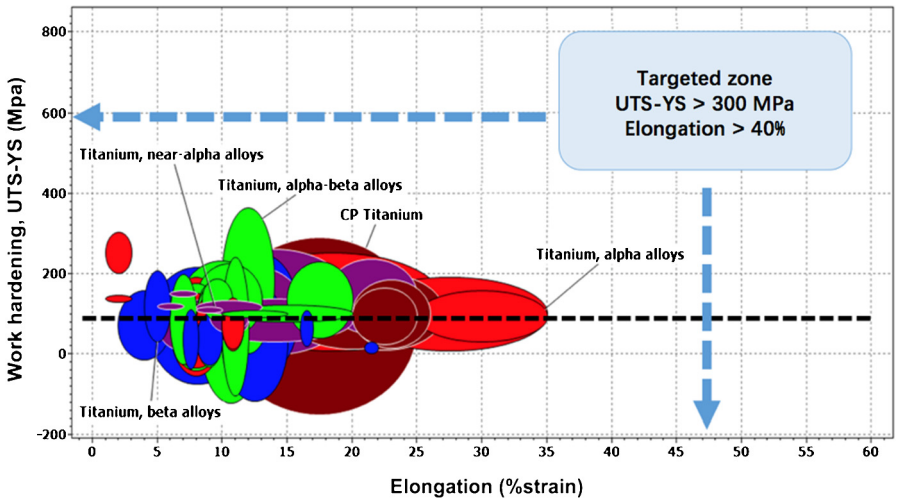

Fig. 5. Diagram plotting the work hardening gain (UTS-YS) as a function of the tensile elongation (%) of conventional titanium alloys in categories β, near-β, α–β, CP Ti, and α. The targeted zone of the designed strain-transformable Ti alloys locates at the upper-right corner of the diagram (UTS-YS > 300 MPa, $E\% > 40\%$).

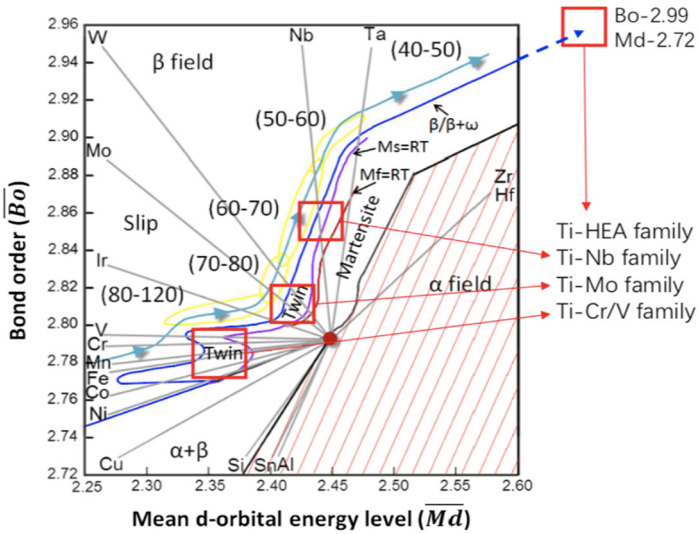

Fig. 6. General $\overline{B_o}$–$\overline{M_d}$ map with individual alloying vectors and four major TWIP/TRIP titanium families.

where X_i is the molar fraction of element i and $(M_d)_i$, $(B_o)_i$ are the numerical values of M_d and B_o for each alloying element, respectively.

After linking the experimental mechanical properties to alloys' B_o–M_d coordinates, a mechanical stability map ($\overline{B_o}$–$\overline{M_d}$ map) was then proposed by Morinaga et al. [62] and later employed by Abdel-Hady et al. [43,63] for predicting the martensitic transformation of Ti-based alloys. An extension of this work has been carried out to produce a general $\overline{B_o}$–$\overline{M_d}$ map adapted for TWIP/TRIP alloys (Fig. 6). As a result, the semi-empirical approach "d-electron alloy design" allowed us to relate the chemical stability of the β phase to the occurrence of specific deformation mechanisms.

Each targeted location in the map could be achieved by a sum of alloying vectors (gray color in Fig. 6) starting from pure Ti (red spot in Fig. 6), which could correspond to several compositions with multi-components. As shown in Fig. 6, the alloying vectors directed towards both up-left and down-left in β region are the β-stabilizing isomorphous elements (e.g., Ta, Nb, W, Mo, V) and the eutectoid elements (e.g., Cr, Fe), respectively. The alloying vectors of the α-stabilizing elements (e.g., Al, Sn) direct downward along the boundary of the $\alpha + \beta$ and α fields, consistently with the previous Mo_{eq} empirical parameter.

In the β field, it can be seen from the map that deformation mechanisms are closely related (in a non-linear way, however) to the β phase chemical stability signed by the two parameters $\overline{B_o}$ and $\overline{M_d}$. The changes of main deformation mechanism mode are shown on the $\overline{B_o}$–$\overline{M_d}$ map based on experimental evidences, illustrated by three main lines (blue, purple and red) in Fig. 6.

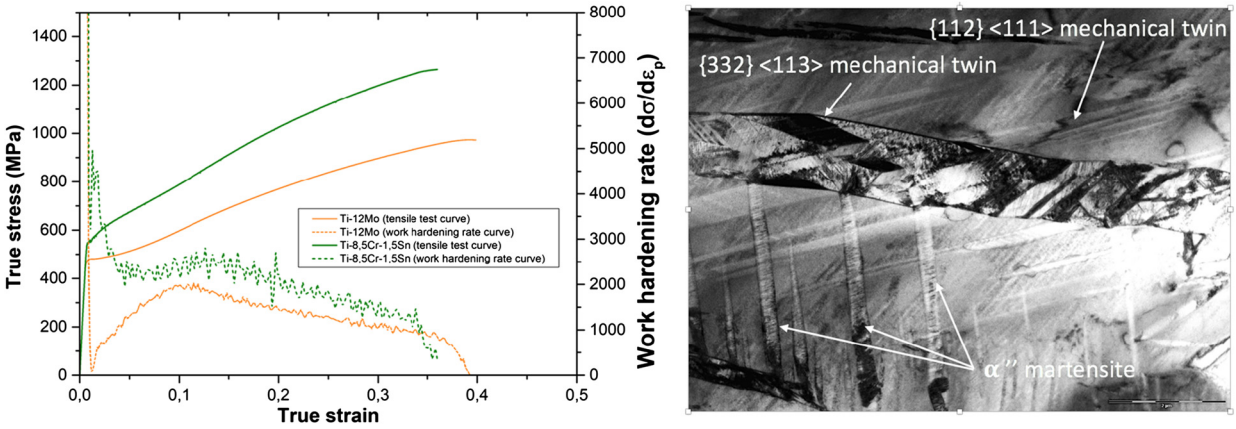

Fig. 7. Tensile true stress–true strain curves and work hardening rates of Ti–12Mo alloy and Ti–8.5Cr–1.5Sn alloy (on the left). The TEM bright field image (on the right) of deformed microstructure (5%) of Ti–12Mo exhibiting both mechanical twins and α″ martensite.

3.3. Some highlights on TRIP/TWIP alloys

The first reports on TWIP/TRIP titanium alloys were published in 2012 [8] and 2013 [9] for a binary Ti–12Mo (wt.%) alloy directly designed from the $\overline{B_o}$–$\overline{M_d}$ map (Fig. 7).

Results from both microstructural (TEM, EBSD, high energy XRD) and mechanical (single and cyclic loading) characterizations validated the design strategy with new alloys displaying a superior combination of strain hardening, strength and ductility, due to the simultaneous occurrence of TRIP/TWIP effects and dislocations slip in the solution-treated state (single phase β). A high nucleation rate of {332}⟨113⟩ mechanical twins, forming a dense network (TWIP), and accompanied by the stress-induced formation of α″ (TRIP) was clearly observed from the onset of plastic deformation. Hypothesis was made that the superior strain hardening observed is actually both a dynamical reduction of the mean free path for dislocations, resulting from the formation of a network of progressively refined twins, and a "dynamical composite effect" resulting from the formation of internal stress fields (back stress) produced by local strain incompatibilities at the twin/matrix interfaces. It was shown that the latter effect results in a marked kinematic strain-hardening behavior.

Considerable work has been performed, since, by different research groups for optimizing the TRIP/TWIP Ti–Mo family, by additional alloying elements [5,10,11,64–70] or by thermomechanical treatments involving precipitation or grain size refinement [5,10,11,64–70], on the one hand, and to extend the design approach to different titanium systems, on the other hand. As an example, compositional optimization has been performed on the Ti–Cr–Sn system in order to achieve a superior combination of mechanical properties from combined TRIP/TWIP effects by introduction, in the design strategy, of a new line $M_d = \mathrm{RT}$ (corresponding to the highest limit of the stress–transformation range) in the stability map, allowing a maximization of the critical stress for SIM transformation, with increased β stabilization. For optimized TRIP/TWIP combined properties, the targeted design zone has to be located around the M_d line, actually corresponding to a transition line between stress-induced transformation and mechanical twinning as the main deformation mechanisms. Mechanical twinning is expected as a favored deformation mechanism on the left side of M_d line whereas stress-induced transformation will occur more and more favorably when approaching the purple line ($M_s = \mathrm{RT}$). The "M_d line approach", as an additional design parameter, brought about several improvements regarding, in particular, both yield strength and strain hardening for the Ti–8.5Cr–1.5Sn alloy, when compared to the first model Ti–12Mo alloy (Fig. 7). This alloy displays, in the solution-treated state, an unusual combination of mechanical properties with a substantial ductility and more than 0.35 of uniform tensile strain, and an impressive strain-hardening effect (equivalent to TWIP steels in normalized hardening rate).

Since then, new fields on the stability map have been explored, with the discovery of a number of new TWIP/TRIP alloys. A summary of the recent researches is shown in Table 1; the selected systems can be divided into four major families: Ti–Mo, Ti–Cr/V, Ti–Nb, and Ti–HEA (locations are indicated in Fig. 6).

Besides and shortly after the development of "first model" alloys such as Ti–Mo and Ti–Mo–W alloys, the question of both applications and industrialization raised quickly, with evident consequences on the choice of the alloying elements among the various possibilities. The excellent compatibility of Cr and V alloying elements to industry-scale Ti production attracted the attention of metal producers, for example.

The quick development of different systems from both Ti–Cr/V and Ti–Nb groups, with the progressive extension of multi-elementary systems (Table 1), can be noted. Interestingly, the "d-electron alloy design" approach could be extended as well to highly concentrated alloys such as High Entropy Alloys (HEAs) [80]; a proof of concept was given that transformation-induced plasticity could be triggered in a BCC refractory high-entropy alloy, Ti35Zr27·5Hf27·5Nb5Ta5, designed from a greatly extended $\overline{B_o}$–$\overline{M_d}$ map, leading to a twofold increase in the normalized work-hardening rate. These two different examples provide quite a strong evidence that this $\overline{B_o}$–$\overline{M_d}$ approach, although much simplified (the location of a given alloy, with respect to the transition lines, is provided from simple vector additions of the elementary alloying vectors) is

Table 1
Summary of the main Ti-based alloys recently investigated.

Alloy family	Compositions (wt.%)	Research groups	Ref.
Ti–Mo	Ti–12Mo	F. Prima; T. Gloriant; P. Jacques	[5,8,9]
	Ti–9Mo–6W	F. Prima; D. Dye	[10,64]
	Ti–10Mo–*x*O	X. Min	[65]
	Ti–10Mo–*x*Fe	K. Tsuchiya	[66]
	Ti–12Mo–5Zr	J.Y. Zhang; F. Prima	[67]
	Ti–15Mo	X. Min; G.H. Cao	[68]
	Ti–15Mo–5Zr	X. Min	[69]
	Ti–15Mo–5W	V. Geanta	[70]
	Ti–16Mo	T. Gloriant	[5]
	Ti–4Al–7Mo–3V–3Cr	S. Sadeghpour	[11]
Ti–Cr/V	Ti–8.5Cr–1.5Sn	F. Prima	[12]
	Ti–4Cr–0.2O	D. Kang; N. Koga	[71]
	Ti–10Cr	M. Niinomi	[72]
	Ti–10V–3Fe–3Al	O.M. Ivasishin; M. Ahmed	[44]
	Ti–10V–3Fe–3Al–0.27O	M. Ahmed	[73]
	Ti–10V–*x*Fe/Cr–3Al	Y.J. Ren; S. van der Zwaag	[74]
	Ti–20V–*x*O	J. Sun	[75]
	Ti–(5-6)Mn–(3-4)Mo	M. Niinomi	[76]
Ti–Nb	Ti–24Nb–*x*(N/O)	T. Gloriant	[17]
	Ti–25Nb–3Zr–3Mo–2Sn	H. Zhan	[77]
	Ti–(36–38)Nb–2Ta–3Zr	D. Raabe	[78]
	Ti–27Nb–0.5Ge	B.S. Lee	[79]
Ti–HEA	Ti35Zr27.5Hf27.5Nb5Ta5	I. Guillot	[80]

actually very robust as a guiding tool for alloy design. Great attention is, however, still needed to be paid to the influence of interstitial elements (such oxygen as addition element) that are not considered in electronic structure calculations, despite their drastic influence on M_s position or on the twinning critical stress, for example.

3.4. Main ongoing discussions and perspectives

If it can be now reasonably considered that both the great interest of TRIP/TWIP alloys (regarding their combination of mechanical properties) and the design approach used to target the suitable titanium systems are somehow validated, the complexity of these strain-transformable alloys still raises a great number of fundamental questions. One of these questions relates to the existing relation between the mechanisms of martensitic transformation and $\{332\}\langle 113\rangle$ twinning after deformation. Various experimental evidences on different systems show that there is probably not a unified sequence of deformation and that the latter could depend on the chemical stability level of the considered alloy. On the less stabilized alloys such as Ti–Nb [47], the system is mainly superelastic, with a high volume fraction of α'' martensite after deformation; the results showed that $\{332\}\langle 113\rangle$ twinning could probably be closely related to the initial stress-induced phase transformation, being potentially a direct product from martensite reversion. In more highly chemically stabilized systems such as Ti–12Mo or Ti–Cr–Sn alloys [12], the initial stress-induced α'' precipitation is much lower; as a consequence, mechanical twinning and martensite precipitation are shown to be quite independent as primary deformation mechanisms, even if α'' precipitation has widely been observed inside $\{332\}\langle 113\rangle$ as a secondary deformation mechanism.

Additionally, one of the principal remaining question deals with the strain-hardening underlying mechanisms. The deformation sequence is shown to be extremely complex in TRIP/TWIP titanium alloys, involving stress-induced precipitation, several types of mechanical twinning ($\{332\}\langle 113\rangle$ and possibly $\{112\}\langle 111\rangle$ types of twins) and a high density of dislocations. As stated before, the chronology of the respective events is still not clear and probably not unique, depending on the alloy. Looking at the mechanical behavior of TWIP steels, it seems highly likely that both a dynamical reduction of the mean free path for dislocations (resulting from the formation of a network of progressively refined twins), and a raising "mechanical contrast" at the twin/matrix interfaces, resulting in the formation of large internal stress fields (back stress) and strong GND (geometrically necessary dislocations) generation, are involved in the high strain-hardening behavior of TRIP/TWIP titanium alloys. However, no quantitative work has been produced so far to estimate the relative effect produced by each mechanism on strain hardening. Besides, the respective effects of grain boundaries and texture on the mechanical behavior of strain-transformable titanium alloys are still to be clarified. In the future work, effort will have to be devoted to the development of constitutive laws dedicated to this family of titanium alloys.

4. Conclusion

The design of new strain-transformable titanium alloys proposed a pathway of discovering novel β metastable compositions with improved elastic and plastic properties for various kinds of applications. Experimental studies confirmed the

design predictions in binary and multi-component systems by showing large superelasticity or unprecedented hardening rate during plastic flow. The deformation mechanisms involving complex martensitic transformations and mechanical twinning are now being investigated by coupling the most advanced experimental methods all over the world. Thanks to the promising potentials of these materials, unsolved fundamental questions such as the physical background of the B_o–M_d model, the origin of {332}⟨113⟩-type twinning, and the heterogeneous martensitic transformations are going back in terms of priority on the research list since their discoveries dating back to the 1980s. The gain of this fundamental knowledge further accelerates the development and spreading of this new family of titanium alloys from scientific researches to industrial applications. Already, new ideas based on the strain-transformable titanium alloys are emerging in terms of strengthening strategy, microstructural control, additive manufacturing, and all aspects for future industrialization. For the incoming years, the proposed design strategy of strain-transformable alloys will support innovation on titanium materials, with new insights on the β metastable microstructural states.

Acknowledgements

The authors acknowledge the European Synchrotron Radiation Facility for provision of synchrotron radiation facilities of the beamline ID22. The authors also acknowledge the THEMIS platform of the University of Rennes (France) for providing access to TEM facilities.

References

[1] G. Lütjering, J.C. Williams, Titanium, Springer, 2007.
[2] S. Banerjee, R. Tewari, G.K. Dey, Omega phase transformation – morphologies and mechanisms, Int. J. Mater. Res. 97 (2006) 963.
[3] F. Prima, et al., Evidence of α-nanophase heterogeneous nucleation from ω particles in a β-metastable Ti-based alloy by high-resolution electron microscopy, Scr. Mater. 54 (2006) 645.
[4] T. Gloriant, et al., Characterization of nanophase precipitation in a metastable β titanium-based alloy by electrical resistivity, dilatometry and neutron diffraction, Scr. Mater. 58 (2008) 271.
[5] F. Sun, F. Prima, T. Gloriant, High-strength nanostructured Ti–12Mo alloy from ductile metastable beta state precursor, Mater. Sci. Eng. A 527 (2010) 4262.
[6] A. Devaraj, et al., Experimental evidence of concurrent compositional and structural instabilities leading to ω precipitation in titanium–molybdenum alloys, Acta Mater. 60 (2012) 596.
[7] D. Choudhuri, et al., Coupled experimental and computational investigation of omega phase evolution in a high misfit titanium–vanadium alloy, Acta Mater. 130 (2017) 215.
[8] M. Marteleur, et al., On the design of new β-metastable titanium alloys with improved work hardening rate thanks to simultaneous TRIP and TWIP effects, Scr. Mater. 66 (2012) 749.
[9] F. Sun, et al., Investigation of early stage deformation mechanisms in a metastable β titanium alloy showing combined twinning-induced plasticity and transformation-induced plasticity effects, Acta Mater. 61 (2013) 6406.
[10] F. Sun, et al., A new titanium alloy with a combination of high strength, high strain hardening and improved ductility, Scr. Mater. 94 (2015) 17.
[11] S. Sadeghpour, S.M. Abbasi, M. Morakabati, Deformation-induced martensitic transformation in a new metastable β titanium alloy, J. Alloys Compd. 650 (2015) 22.
[12] C. Brozek, et al., A β-titanium alloy with extra high strain-hardening rate: design and mechanical properties, Scr. Mater. 114 (2016) 60.
[13] H.Y. Kim, et al., Martensitic transformation, shape memory effect and superelasticity of Ti–Nb binary alloys, Acta Mater. 54 (2006) 2419.
[14] E. Bertrand, et al., Synthesis and characterisation of a new superelastic Ti–25Ta–25Nb biomedical alloy, J. Mech. Behav. Biomed. Mater. 3 (2010) 559.
[15] E. Bertrand, P. Castany, T. Gloriant, Investigation of the martensitic transformation and the damping behavior of a superelastic Ti–Ta–Nb alloy, Acta Mater. 61 (2013) 511.
[16] Q. Li, et al., Effect of Zr on super-elasticity and mechanical properties of Ti-24 at% Nb-(0, 2, 4) at% Zr alloy subjected to aging treatment, Mater. Sci. Eng. A 536 (2012) 197.
[17] P. Castany, et al., In situ synchrotron X-ray diffraction study of the martensitic transformation in superelastic Ti–24Nb–0.5N and Ti–24Nb–0.5O alloys, Acta Mater. 88 (2015) 102.
[18] Y. Yang, et al., Characterization of the martensitic transformation in the superelastic Ti–24Nb–4Zr–8Sn alloy by in situ synchrotron X-ray diffraction and dynamic mechanical analysis, Acta Mater. 88 (2015) 25.
[19] J.K. Bass, H. Fine, G.J. Cisneros, Nickel hypersensitivity in the orthodontic patient, Am. J. Orthod. Dentofac. Orthop. 103 (1993) 280.
[20] H. Kerosuo, et al., Nickel allergy in adolescents in relation to orthodontic treatment and piercing of ears, Am. J. Orthod. Dentofac. Orthop. 109 (1996) 148.
[21] H.H. Huang, et al., Ion release from NiTi orthodontic wires in artificial saliva with various acidities, Biomaterials 24 (2003) 3585.
[22] H.Y. Kim, et al., Effect of Ta addition on shape memory behavior of Ti–22Nb alloy, Mater. Sci. Eng. A 417 (2006) 120.
[23] J.I. Kim, et al., Shape memory characteristics of Ti–22Nb–(2–8)Zr(at.%) biomedical alloys, Mater. Sci. Eng. A 403 (2005) 334.
[24] F. Sun, et al., Influence of a short thermal treatment on the superelastic properties of a titanium-based alloy, Scr. Mater. 63 (2010) 1053.
[25] F. Sun, et al., A thermo-mechanical treatment to improve the superelastic performances of biomedical Ti–26Nb and Ti–20Nb–6Zr (at.%) alloys, J. Mech. Behav. Biomed. Mater. 4 (2011) 1864.
[26] Y. Yang, et al., Texture investigation of the superelastic Ti–24Nb–4Zr–8Sn alloy, J. Alloys Compd. 591 (2014) 85.
[27] H. Jabir, et al., Cristallographic orientation dependence of mechanical properties in the superelastic Ti–24Nb–4Zr–8Sn, Phys. Rev. Mater. (2018), submitted.
[28] H.Y. Kim, et al., Texture and shape memory behavior of Ti–22Nb–6Ta alloy, Acta Mater. 54 (2006) 423.
[29] M.F. Ijaz, et al., Superelastic properties of biomedical (Ti–Zr)–Mo–Sn alloys, Mater. Sci. Eng. C 48 (2015) 11.
[30] M. Tahara, et al., Cyclic deformation behavior of a Ti-26 at.% Nb alloy, Acta Mater. 57 (2009) 2461.
[31] E.G. Obbard, et al., Mechanics of superelasticity in Ti–30Nb–(8–10)Ta–5Zr alloy, Acta Mater. 58 (2010) 3557.
[32] A. Ramarolahy, et al., Microstructure and mechanical behavior of superelastic Ti–24Nb–0.5O and Ti–24Nb–0.5N biomedical alloys, J. Mech. Behav. Biomed. Mater. 9 (2012) 83.
[33] M. Tahara, et al., Lattice modulation and superelasticity in oxygen-added β-Ti alloys, Acta Mater. 59 (2011) 6208.

[34] P. Castany, M. Besse, T. Gloriant, Dislocation mobility in gum metal beta-titanium alloy studied via in situ transmission electron microscopy, Phys. Rev. B 84 (2011) 020201.
[35] M. Besse, P. Castany, T. Gloriant, Mechanisms of deformation in gum metal TNTZ–O and TNTZ titanium alloys: a comparative study on the oxygen influence, Acta Mater. 59 (2011) 5982.
[36] P. Castany, M. Besse, T. Gloriant, In situ TEM study of dislocation slip in a metastable β titanium alloy, Scr. Mater. 66 (2012) 371.
[37] P. Castany, et al., Deformation mechanisms and biocompatibility of the superelastic Ti–23Nb–0.7Ta–2Zr–0.5N alloy, Shape Mem. Superelasticity 2 (2016) 18.
[38] Y. Kamimura, et al., Thermally activated deformation of gum metal: a strong evidence for the Peierls mechanism of deformation, Mater. Trans. 56 (2015) 2084.
[39] E. Plancher, et al., On dislocation involvement in Ti–Nb gum metal plasticity, Scr. Mater. 68 (2013) 805.
[40] D.C. Chrzan, et al., Spreading of dislocation cores in elastically anisotropic body-centered-cubic materials: the case of gum metal, Phys. Rev. B 82 (2010) 184202.
[41] J. Huang, H. Xing, J. Sun, Structural stability and generalized stacking fault energies in β Ti–Nb alloys: relation to dislocation properties, Scr. Mater. 66 (2012) 682.
[42] S. Hanada, O. Izumi, Transmission electron microscopic observations of mechanical twinning in metastable beta titanium alloys, Metall. Trans. A 17 (1986) 1409.
[43] M. Abdel-Hady, K. Hinoshita, M. Morinaga, General approach to phase stability and elastic properties of β-type Ti-alloys using electronic parameters, Scr. Mater. 55 (2006) 477.
[44] M. Ahmed, et al., The influence of β phase stability on deformation mode and compressive mechanical properties of Ti–10V–3Fe–3Al alloy, Acta Mater. 84 (2015) 124.
[45] E. Bertrand, et al., Twinning system selection in a metastable β-titanium alloy by Schmid factor analysis, Scr. Mater. 64 (2011) 1110.
[46] M.J. Blackburn, J.A. Feeney, Stress-induced transformations in Ti–Mo alloys, J. Inst. Met. 99 (1971) 132.
[47] P. Castany, et al., Reversion of a parent $\{130\}\langle 310\rangle_{\alpha''}$ martensitic twinning system at the origin of $\{332\}\langle 113\rangle_{\beta}$ twins observed in metastable beta titanium alloys, Phys. Rev. Lett. 117 (2016) 245501.
[48] E. Bertrand, et al., Deformation twinning in the full-α'' martensitic Ti–25Ta–20Nb shape memory alloy, Acta Mater. 105 (2016) 94.
[49] M. Tahara, et al., Plastic deformation behaviour of single-crystalline martensite of Ti–Nb shape memory alloy, Sci. Rep. 7 (2017) 15715.
[50] Y. Yang, et al., Stress release-induced interfacial twin boundary ω phase formation in a β type Ti-based single crystal displaying stress-induced α'' martensitic transformation, Acta Mater. 149 (2018) 97.
[51] J. Fu, et al., Novel Ti-base superelastic alloys with large recovery strain and excellent biocompatibility, Acta Biomater. 17 (2015) 56.
[52] M.F. Ijaz, et al., Design of a novel superelastic Ti–23Hf–3Mo–4Sn biomedical alloy combining low modulus, high strength and large recovery strain, Mater. Lett. 177 (2016) 39.
[53] A. Ramalohary, et al., Superelastic property induced by low-temperature heating of a shape memory Ti–24Nb–0.5Si biomedical alloy, Scr. Mater. 88 (2014) 25.
[54] R. Boyer, Aerospace applications of beta titanium alloys, JOM 46 (1994) 20.
[55] P.J. Winkler, M.A. Äubler, M. Peters, Application of Ti alloys in the European aerospace industry, in: Titanium' 92 Science and Technology, Proceedings of a Symposium Sponsored by the Titanium Committee of the Minerals, Metals and Materials Structural Metals Division Held at the World Titanium Conference (7th), San Diego, California, June 29–July 2, 1992, p. 2877.
[56] P.J. Bania, Beta titanium alloys and their role in the titanium industry, JOM 46 (1994) 16.
[57] M. Morinaga, et al., Theoretical design of titanium alloys, in: P. Lacombe, R. Tricot, G. Béranger (Eds.), Sixth World Conference on Titanium, Cannes, June 6–9, 1988, vol. III, Les Éditions de Physique, 1989, p. 1601.
[58] D. Kuroda, et al., Design and mechanical properties of new β type titanium alloys for implant materials, Mater. Sci. Eng. A 243 (1998) 244.
[59] M. Morinaga, H. Adachi, M. Tsukada, Electronic structure and phase stability of ZrO_2, J. Phys. Chem. Solids 44 (1983) 301.
[60] M. Morinaga, et al., New PHACOMP and its applications to alloy design, Superalloys 1984 (1984) 523.
[61] M. Morinaga, et al., Solid solubilities in transition-metal-based fcc alloys, Philos. Mag. A 51 (1985) 223.
[62] M. Morinaga, et al., Theoretical design of β-type titanium alloys, in: Science and Technology, Proceedings of the 7th International Conference on Titanium, 1992, p. 276.
[63] M. Abdel-Hady, et al., Phase stability change with Zr content in β-type Ti–Nb alloys, Scr. Mater. 57 (2007) 1000.
[64] J. Gao, et al., Segregation mediated heterogeneous structure in a metastable β titanium alloy with a superior combination of strength and ductility, Sci. Rep. 8 (2018) 7512.
[65] X. Min, et al., Effect of oxygen content on deformation mode and corrosion behavior in β-type Ti–Mo alloy, Mater. Sci. Eng. A 684 (2017) 534.
[66] I. Gutierrez-Urrutia, C.-L. Li, K. Tsuchiya, $\{332\}\langle 113\rangle$ detwinning in a multilayered bcc-Ti–10Mo–Fe alloy, J. Mater. Sci. 52 (2017) 7858.
[67] J. Zhang, et al., Fabrication and characterization of a novel β metastable Ti–Mo–Zr alloy with large ductility and improved yield strength, Mater. Charact. 139 (2018) 421.
[68] X. Min, et al., Mechanical twinning and dislocation slip multilayered deformation microstructures in β-type Ti–Mo base alloy, Scr. Mater. 102 (2015) 79.
[69] X. Zhou, X. Min, Effect of grain boundary angle on $\{332\}\langle 113\rangle$ twinning transfer behavior in β-type Ti–15Mo–5Zr alloy, J. Mater. Sci. 53 (2018) 8604.
[70] M. Buzatu, et al., Obtaining and characterization of the Ti15Mo5W alloy for biomedical applications, Mater. Plast. 54 (2017) 596.
[71] D.-S. Kang, et al., Enhanced work hardening by redistribution of oxygen in $(\alpha+\beta)$-type Ti–4Cr–0.2O alloys, Mater. Sci. Eng. A 606 (2014) 101.
[72] M. Niinomi, Enhancement of mechanical biocompatibility of titanium alloys by deformation-induced transformation, Mater. Sci. Forum 879 (2017).
[73] M. Ahmed, et al., Stress-induced twinning and phase transformations during the compression of a Ti–10V–3Fe–3Al alloy, Metall. Mater. Trans. A 48 (2017) 2791.
[74] C. Li, et al., Effect of strain rate on stress-induced martensitic formation and the compressive properties of Ti–V–(Cr, Fe)–Al alloys, Mater. Sci. Eng. A 573 (2013) 111.
[75] X.L. Wang, et al., Role of oxygen in stress-induced ω phase transformation and $\{332\}\langle 113\rangle$ mechanical twinning in β Ti–20V alloy, Scr. Mater. 96 (2015) 37.
[76] P. Fernandes Santos, et al., Improvement of microstructure, mechanical and corrosion properties of biomedical Ti–Mn alloys by Mo addition, Mater. Des. 110 (2016) 414.
[77] H. Zhan, et al., On the deformation mechanisms and strain rate sensitivity of a metastable β Ti–Nb alloy, Scr. Mater. 107 (2015) 34.
[78] M.J. Lai, C.C. Tasan, D. Raabe, On the mechanism of {332} twinning in metastable β titanium alloys, Acta Mater. 111 (2016) 173.
[79] B.-S. Lee, et al., Stress-induced α'' martensitic transformation mechanism in deformation twinning of metastable β-type Ti–27Nb–0.5Ge alloy under tension, Mater. Trans. 57 (2016) 1868.
[80] L. Lilensten, et al., Design and tensile properties of a bcc Ti-rich high-entropy alloy with transformation-induced plasticity, Mater. Res. Lett. 5 (2017) 110.